Heterogeneous Catalysis

DOI: 10.1002/anie.200803574

A Reactive Oxide Overlayer on Rhodium Nanoparticles during CO Oxidation and Its Size Dependence Studied by In Situ Ambient-Pressure X-ray Photoelectron Spectroscopy**

*Michael E. Grass, Yawen Zhang, Derek R. Butcher, Jeong Y. Park, Yimin Li, Hendrik Bluhm, Kaitlin M. Bratlie, Tianfu Zhang, and Gabor A. Somorjai**

Carbon monoxide oxidation is one of the most studied heterogeneous reactions, being scientifically and industrially important, particularly for removal of CO from exhaust streams[1] and preferential oxidation for hydrogen purification in fuel-cell applications.[2] The precious metals Ru, Rh, Pd, Pt, and Au are most commonly used for this reaction because of their high activity and stability. Despite the wealth of experimental and theoretical data, it remains unclear what is the active surface for CO oxidation under catalytic conditions for these metals. Herein we utilize in situ synchrotron ambient pressure X-ray photoelectron spectroscopy (APXPS) to monitor the oxidation state at the surface of rhodium nanoparticles (Rh NPs) during CO oxidation and demonstrate that the active catalyst is a surface oxide, the formation of which is dependent on particle size. The amount of oxide formed and the reaction rate both increase with decreasing particle size.

Many single-crystal CO oxidation studies over rhodium suggest that the reaction is structure-insensitive and that the oxide formation decreases the reaction rate.[3,4] However, recent advances in synthetic techniques and in-situ experimentation have revealed that the oxidation state and stoichiometry of the surface oxide greatly affects CO oxidation rates.[5–9] At low temperatures or low O_2/CO ratios, CO strongly adsorbs onto the catalyst surface and inhibits O_2 adsorption. At high temperatures or high O_2/CO ratios, the catalyst surface becomes saturated with oxygen atoms and the reaction proceeds more rapidly. It has been demonstrated that small palladium nanoparticles[6] are more active for CO oxidation than larger particles and single crystals, whereas the opposite is reported for platinum.[10] For Rh NPs, no particle size effect was observed for supported rhodium catalysts,[11] but a strong particle size dependence was observed for CO desorption, dissociation, and transient CO oxidation over electron-beam-prepared Rh NPs that were precovered with oxygen.[12,13]

For this investigation we have prepared small, polymer-stabilized Rh NPs with a narrow size distribution and studied CO oxidation; polymer stabilized NP syntheses enable control of NP size, shape, and/or composition for reaction studies.[14,15] The turnover frequency (TOF) for CO oxidation at 200 °C increases five-fold, and the apparent activation energy decreases from 27.9 kcal mol^{-1} to 19.0 kcal mol^{-1} as the particle size decreases from 11 nm to 2 nm. APXPS of 2 nm and 7 nm Rh NP films during CO oxidation at about 1 Torr provides the first in-situ measurement of the oxidation state of Rh NPs during CO oxidation and demonstrates that smaller particles are more oxidized than larger particles during reaction at 150–200 °C. A surface oxygen species is also observed during CO oxidation that is not present when heating in O_2 alone, possibly indicating a unique active oxide phase on Rh NPs. This oxide phase may alter the relative bonding geometries of CO and/or oxygen on the rhodium surface, thereby lowering the activation energy for the reaction.[16]

The synthesis of monodisperse Rh NPs by polyol reduction using poly(vinylpyrrolidone) (PVP) as a capping agent and [Rh(acac)$_3$] as a rhodium precursor[17] was extended to smaller sizes by the addition of sodium citrate. Using this approach, Rh NPs of 3.5 nm (3.6 ± 0.5 nm), 2.5 nm (2.5 ± 0.4 nm), and 2 nm (1.9 ± 0.3 nm) were formed by increasing the amount of sodium citrate. Monolayer films of these particles were then prepared in a Langmuir–Blodgett (LB) trough and characterized with transmission electron microscopy (TEM) and XPS. Figure 1 a–c shows TEM images of the NPs, with insets of size distribution histograms taken from 100 particles. Figure 1 f shows X-ray photoelectron spectra for the Rh 3d peak of the as-synthesized (no pretreatment) particles after LB deposition onto a silicon wafer. The ratio of oxidized rhodium to reduced rhodium clearly increases as the particle size decreases.

The three samples of small Rh NP (2, 2.5, and 3.5 nm) LB films and two previously synthesized samples, 7 nm ($7.1 \pm$

[*] M. E. Grass, D. R. Butcher, Dr. J. Y. Park, Dr. Y. Li, Dr. H. Bluhm, Dr. K. M. Bratlie, Dr. T. Zhang, Prof. G. A. Somorjai
Department of Chemistry; University of California, Berkeley
Chemical and Materials Sciences Divisions
Lawrence Berkeley National Laboratory; Berkeley, CA 94720 (USA)
Fax: (+1) 510-643-9668
E-mail: Somorjai@berkeley.edu
Prof. Y. Zhang
College of Chemistry and Molecular Engineering
Peking University, Beijing 100871 (P.R. China)

[**] This work was supported by the Director, Office of Science, Office of Advanced Scientific Computing Research, Office of Basic Energy Sciences, Materials Sciences and Engineering, and Chemical Sciences, Geosciences, and Biosciences Division of the U.S. Department of Energy under Contract Nos. DE-AC02-05CH11231 and DE-AC03-76SF00098. We also thank the Molecular Foundry and the Advanced Light Source, LBNL for use of their facilities and Prof. Miquel Salmeron and Dr. Zhi Liu for valuable discussions. Y.W.Z. appreciates financial aid with a Huaxin Distinguished Scholar Award from Peking University Education Foundation of China.

Supporting information for this article is available on the WWW under http://dx.doi.org/10.1002/anie.200803574.

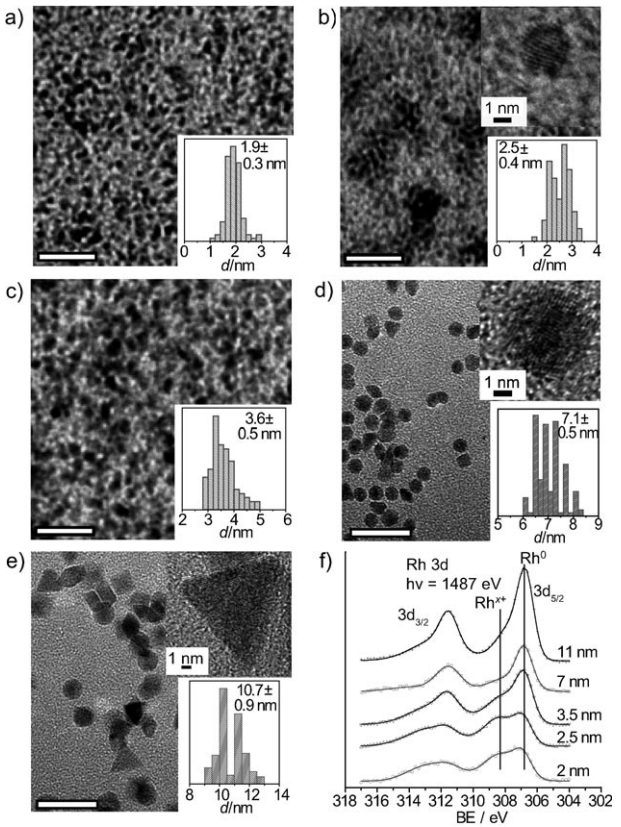

Figure 1. TEM images with insets of particle size distribution histograms of 100 particles for a) 2 nm, b) 2.5 nm, c) 3.5 nm, d) 7 nm, and e) 11 nm Rh NPs. All scale bars are 20 nm except for the HRTEM insets. f) Rh 3d XPS spectra of the 2, 2.5, and 3.5 nm Rh NPs together with previously synthesized 7 and 11 nm Rh NPs, showing the increase in oxidized rhodium as the particle size decreases.

0.5 nm) and 11 nm (10.7 ± 0.9 nm) LB films (Figure 1 d, e) were tested for catalytic activity in CO oxidation by O_2 in a batch reactor monitored with a gas chromatograph. The pressures of CO and O_2 were 20 Torr and 50 Torr, respectively, with a back pressure of helium to reach 900 Torr. The activity was measured at 150, 175, 200, and 225 °C to determine the apparent activation energy. Figure 2 a shows the TOF and apparent activation energy of the five samples relative to a rhodium foil. A description of the calculation of surface rhodium atoms for the calculation of TOF can be found in the Supporting Information. The TOF increases from 5.5 for the reaction over 11 nm Rh NPs to 28.0 for the reaction over 2 nm Rh NPs at 200 °C relative to a rhodium foil ($0.28\ s^{-1}$). The apparent activation energy concurrently decreases from 27.9 kcal mol^{-1} to 19.0 kcal mol^{-1}. Both the TOF and the apparent activation energy fit to an exponential, which is consistent with the thermodynamics of oxide stability for nanoparticles as a function of size [see Eq. (1)].

After multiple cycles of CO oxidation between 150 and 225 °C, none of the samples exhibited a change in TOF or activation energy. At temperatures above 250 °C, significant deactivation was observed and SEM images after reaction showed a high degree of sintering; these higher temperatures were not included in this investigation. PVP and/or its decomposition products may play an important role in stabilizing the nanoparticles against sintering or dispersion at temperatures below 250 °C. Above 250 °C much of the PVP has likely decomposed (Supporting Information, Figure S5) and the particles easily sinter. The 7 and 11 nm NP samples were checked before and after reaction and no changes in morphology or particle sintering were observed (Supporting Information, Figure S7). Many IR spectroscopy studies have demonstrated that isolated $Rh^I(CO)_2$ sites can form in the presence of CO[18–20] or during reaction, but these sites are inactive for CO oxidation.[18,19] In an ongoing investigation of these same Rh NPs supported on a high-surface-area SiO_2 catalyst support, we have not observed the formation of $Rh^I(CO)_2$ in the presence of CO between room temperature and 200 °C. These data will be published later. Based on these results and the fact that we do not observe any decrease in activity of the 2 nm NPs after repeated reaction cycles, it appears that the Rh NPs of all sizes are stable up to 225 °C during reaction.

APXPS was carried out at the Advanced Light Source Beamline 11.0.2, LBNL,[21] using the same LB films described above. The photon energy of the X-ray source was tuned such that the kinetic energy of the detected electrons for all the spectra was centered at circa 190 eV. The experimental procedure for each sample consisted of introducing 200 mTorr CO and acquiring spectra at 25, 100, 150, and 200 °C (ca. 30 min. at each temperature), then cooling and evacuating the chamber (ca. 10^{-8} Torr). 500 mTorr O_2 was

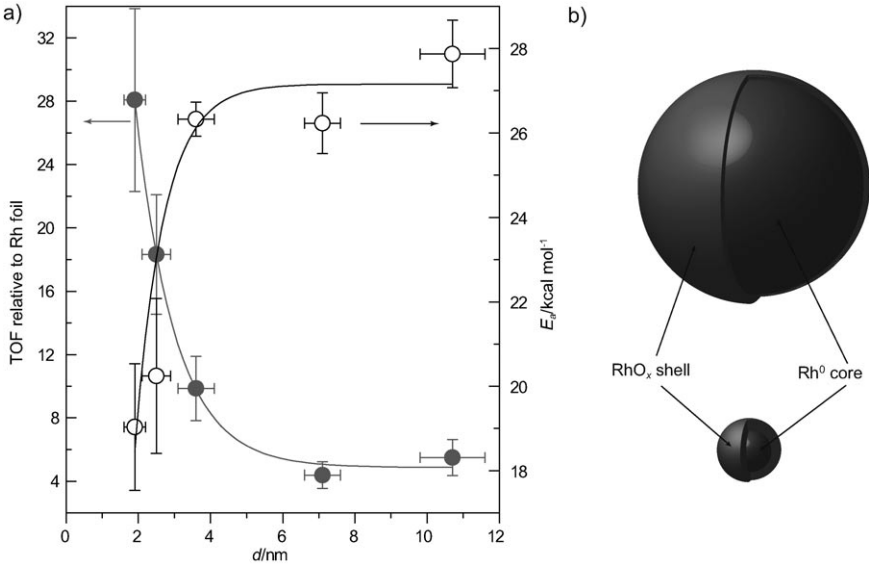

Figure 2. a) Turnover frequency relative to rhodium foil at 50 Torr O_2, 20 Torr CO, at 200 °C, and activation energy (150–225 °C) for CO oxidation. b) The thickness of the oxide shell scales with particle size; 2 nm and 7 nm NPs are illustrated here with the oxide layers shown to scale, as determined by APXPS.

then introduced and the heating process was repeated. Finally, 200 mTorr CO and 500 mTorr O_2 were introduced together and heated. As a result of the experimental setup, equilibrium pressures of about 20 mTorr for CO, 180 mTorr for CO_2, and 410 mTorr for O_2 were established under the reaction conditions. The spectra obtained during heating in CO or O_2 alone, along with the procedures for fitting spectra, are discussed in the Supporting Information.

The Rh 3d spectra in the presence of CO (200 mTorr) and O_2 (500 mTorr) at 150 and 200 °C are shown in Figure 3. The NPs of both samples are initially oxidized because they were previously exposed to O_2 at 200 °C; the surface of the 7 nm NPs are 54 % Rh^{x+} and the 2 nm NPs are 70 % Rh^{x+} when CO and O_2 are first introduced into the chamber. Both samples reduce in the reaction mixture, with the amount of Rh^{x+} decreasing to 8 % for the 7 nm NPs and to 43 % for the 2 nm NPs at 150 °C.

Continued heating, however, results in reoxidation of the rhodium surface, indicating that the coverage of CO on the NP surface decreases and there is a simultaneous increase in oxygen coverage. The fraction of Rh^{x+} increases to 25 % for the 7 nm NPs and to 67 % for the 2 nm NPs at 200 °C. These data suggest that the active phase for CO oxidation is a surface oxide. It also provides in situ evidence that smaller NPs more readily form this surface oxide under reaction conditions, which is consistent with TOF and activation energy measurements (Figure 2 a). The nature of the oxide phase is not within the scope of this work, and it may be affected by the presence of the PVP capping layer that surrounds these particles. For both NP systems, however, the particles are not completely oxidized and thus there must be an interface between the oxide surface and the metallic core. The presence of this interface induces a strain on the oxide which makes it less stable and thus more reactive.[5] An additional strain may also be induced from the small size of nanoparticles, which distorts the bonding of surface atoms. This increased instability may be an added reason for the higher reactivity of the smaller NPs.

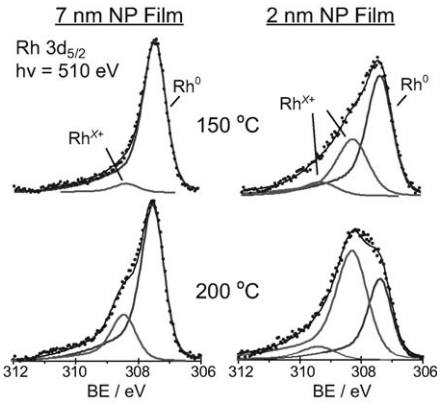

Figure 3. APXPS spectra of the Rh $3d_{5/2}$ peak, with fits for reduced rhodium (307.2 eV) and oxidized rhodium (308.2 eV, 309.4 eV). The NPs of both films (2 nm and 7 nm particles) at higher temperatures are more oxidized compared to their initial state. Compared to the film that is comprised of 7 nm, the 2 nm NPs are more oxidized at all temperatures. The two Rh^{x+} peaks are attributed to rhodium atoms in two different oxidation states or coordinated to a different number of oxygen atoms.

If the mean free path (MFP) of the photoelectrons is taken to be 0.5 nm,[22] then the thickness of the oxide layer formed can be roughly estimated by considering the nanoparticles as spheres and the XPS intensity from each layer decreasing exponentially with depth. For example, for a 1.9 nm NP, the first layer comprises 52 % of the atoms and 67 % of the XPS intensity and the second layer comprises 30 % of the atoms and 25 % of the XPS intensity. Using this method, the oxide overlayer is estimated to be 0.6 of a layer, 1, and 1.6 layers for the 2 nm NPs at 150, 200, and 275 °C, respectively. For the 7 nm NPs, there is only 0.2 and 0.6 of a layer at 150 and 200 °C, respectively, indicating incomplete oxide formation of even a single layer over the larger NPs. A comparison of the two samples at 200 °C is illustrated to scale in Figure 2 b.

Under the conditions of these experiments, the oxygen chemical potential is high enough that the bulk oxide is thermodynamically stable ($\mu_0 = -0.36$ eV at 25 °C, -0.62 eV at 200 °C), but it has been shown that for rhodium single crystals under similar temperatures and pressures, the oxide formation is kinetically controlled.[23] Although this system is also likely under kinetic control, it is instructive to understand how NP size affects oxide stability. A simple thermodynamic model for nanoparticles, similar to that developed for thin films,[24] has been formulated and used to understand the dissociation pressure of a RhO_2 NP as a function of particle size (see the Supporting Information):

$$P_{O_2}^{NP} = P_{O_2}^{bulk} \exp\left(-\frac{21\ \text{nm}}{r_0}\right) \quad (1)$$

where P is the dissociation pressure of a RhO_2 NP and r_0 is the size of the corresponding metal Rh NP. From this equation, the dissociation pressure of a 7 nm RhO_2 NP is 20 times lower than that of the bulk, whereas for a 2 nm Rh NP, the dissociation pressure is decreased by a factor of 4×10^4.

Along with the increase in the amount of oxidized rhodium species observed in the Rh 3d spectra at 200 °C under reaction conditions with CO, a low binding energy peak (at ca. 529.5 eV) in the O 1s spectrum is also observed (Figure 4 b and d) that is not present during heating in O_2 alone (Figure 4 a and c). This suggests that a distinct oxide forms during CO oxidation that is stabilized by CO or a reaction intermediate and does not form when the NPs are simply heated in O_2.[5] The peak associated with this "reactive oxide" overlayer diminishes upon evacuation of the reaction chamber, further establishing that this oxide is intimately correlated with the CO oxidation reaction. Most of the O 1s intensity associated with surface oxygen (peak centered at ca. 531 eV) is attributed to PVP. Further characterization of this oxide and its size dependence is necessary, and may enhance theoretical models for understanding nanoparticle activity as a function of metal type and particle size. Gas-phase O_2, CO, and CO_2 are also observed in Figure 4, and we will utilize this added information in future studies after designing a sample holder that does not itself exhibit catalytic activity.

In a recent theoretical study, Gong et al. carried out DFT calculations for $CO + O \rightarrow CO_2$ on metal and oxide surfaces, including Rh(111), and found that the reaction barrier is

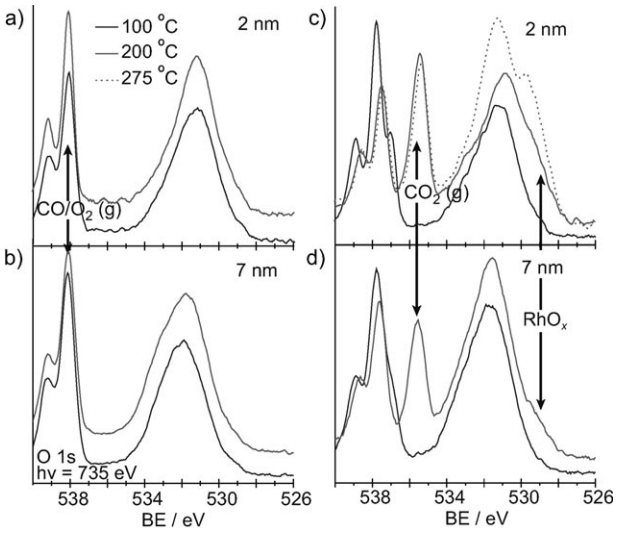

Figure 4. O 1s spectra of 2 nm and 7 nm Rh NPs in 500 mTorr O_2 (a and c) and during reaction (410 mTorr O_2, 20 mTorr CO; b and d). When exposed to both O_2 and CO, a peak at higher binding energy forms, which is attributed to a RhO_x species.

lower over the oxide than over the metal because of a change in the adsorption geometry of oxygen atoms.[16] Herein, we have directly correlated the amount of surface oxide on two different sizes of Rh NPs with the TOF and apparent activation energy. The observed particle size dependence of CO oxidation over Rh NPs in this study is correlated with increased oxide formation over small particles. PVP may also play a role in the formation of the surface oxide layer and affect the interaction of CO and O_2 with the Rh surface.

In-situ studies are invaluable to the understanding of a working catalyst, and we had demonstrated the first observation of the active phase of a Rh NP catalyst during CO oxidation by photoelectron spectroscopy, providing evidence for the observed size dependence of this reaction. Further studies are required to understand the form of the reactive oxide and the role, if any, of PVP in its formation. Importantly, this study shows that the use of APXPS in the study of model catalysts will be able to complement other in-situ techniques, such as scanning tunneling microscopy and surface X-ray diffraction, in determining the structure of a catalyst during reactions.

Experimental Section

The synthesis of 7 and 11 nm Rh NPs and Langmuir–Blodgett (LB) films has been described elsewhere.[17] The setup of the chamber and the sample holder has also been explained in detail.[21] Synthesis of 2 nm Rh NPs: $[Rh(acac)_3]$ (0.1 mmol), sodium citrate (0.3 mmol), and poly(vinylpyrrolidone) (PVP, 55 K, molarity in terms of monomer units; 1 mmol), were added to 1,4-butanediol (20 mL) in a 50 mL three-necked flask at room temperature. The stock solution was heated to 140 °C in a Glas-Col electromantle (60 W; 50 mL) with a Cole–Parmer temperature controller (Diqi-sense), and the flask was evacuated at this temperature for 20 min to remove water and oxygen under magnetic stirring, resulting in an optically transparent orange-yellow solution. The flask was then heated to 220 °C at a rate of 10 °C min^{-1}, and maintained at this temperature (±2 °C) for 2 h under argon. During the reaction, the color of the solution gradually turned from orange-yellow to black. When the reaction was complete, an excess of acetone was poured into the solution at room temperature to form a cloudy black suspension. This suspension was separated by centrifugation at 4200 rpm for 6 min, and the black product was collected by discarding the colorless supernatant. The precipitated Rh NPs were washed with acetone once, and then redispersed in ethanol. The 2.5 and 3.5 nm Rh NPs were synthesized similarly using sodium citrate (0.1 mmol and 0.025 mmol, respectively).

Received: July 22, 2008
Published online: October 16, 2008

Keywords: carbon monoxide · heterogeneous catalysis · nanomaterials · rhodium · XPS

[1] J. T. Kummer, *J. Phys. Chem.* **1986**, *90*, 4747.
[2] L. Carrette, K. A. Friedrich, U. Stimming, *ChemPhysChem* **2000**, *1*, 162.
[3] P. J. Berlowitz, C. H. F. Peden, D. W. Goodman, *J. Phys. Chem.* **1988**, *92*, 5213.
[4] C. H. F. Peden, D. W. Goodman, D. S. Blair, P. J. Berlowitz, G. B. Fisher, S. H. Oh, *J. Phys. Chem.* **1988**, *92*, 1563.
[5] M. D. Ackermann, T. M. Pedersen, B. L. M. Hendriksen, O. Robach, S. C. Bobaru, I. Popa, C. Quiros, H. Kim, B. Hammer, S. Ferrer, J. W. M. Frenken, *Phys. Rev. Lett.* **2005**, *95*, 255505.
[6] M. S. Chen, Y. Cal, Z. Yan, K. K. Gath, S. Axnanda, D. W. Goodman, *Surf. Sci.* **2007**, *601*, 5326.
[7] H. Gabasch, A. Knop-Gericke, R. Schlogl, M. Borasio, C. Weilach, G. Rupprechter, S. Penner, B. Jenewein, K. Hayek, B. Klotzer, *Phys. Chem. Chem. Phys.* **2007**, *9*, 533.
[8] T. Schalow, B. Brandt, M. Laurin, S. Schauermann, J. Libuda, H. J. Freund, *J. Catal.* **2006**, *242*, 58.
[9] B. L. M. Hendriksen, J. W. M. Frenken, *Phys. Rev. Lett.* **2002**, *89*, 046101.
[10] M. Herskowitz, R. Holliday, M. B. Cutlip, C. N. Kenney, *J. Catal.* **1982**, *74*, 408.
[11] S. H. Oh, C. C. Eickel, *J. Catal.* **1991**, *128*, 526.
[12] V. Nehasil, I. Stara, V. Matolin, *Surf. Sci.* **1995**, *331–333*, 105.
[13] V. Nehasil, I. Stara, V. Matolin, *Surf. Sci.* **1996**, *352*, 305.
[14] R. Narayanan, M. A. El-Sayed, *J. Am. Chem. Soc.* **2003**, *125*, 8340.
[15] J. Y. Park, Y. Zhang, M. Grass, T. Zhang, G. A. Somorjai, *Nano Lett.* **2008**, *8*, 673.
[16] X. Q. Gong, Z. P. Liu, R. Raval, P. Hu, *J. Am. Chem. Soc.* **2004**, *126*, 8.
[17] Y. W. Zhang, M. E. Grass, S. E. Habas, F. Tao, T. F. Zhang, P. D. Yang, G. A. Somorjai, *J. Phys. Chem. C* **2007**, *111*, 12243.
[18] J. A. Anderson, *J. Chem. Soc. Faraday Trans.* **1991**, *87*, 3907.
[19] M. Cavers, J. M. Davidson, I. R. Harkness, L. V. C. Rees, G. S. McDougall, *J. Catal.* **1999**, *188*, 426.
[20] C. A. Rice, S. D. Worley, C. W. Curtis, J. A. Guin, A. R. Tarrer, *J. Chem. Phys.* **1981**, *74*, 6487.
[21] H. Bluhm, K. Andersson, T. Araki, K. Benzerara, G. E. Brown, J. J. Dynes, S. Ghosal, M. K. Gilles, H. C. Hansen, J. C. Hemminger, A. P. Hitchcock, G. Ketteler, A. L. D. Kilcoyne, E. Kneedler, J. R. Lawrence, G. G. Leppard, J. Majzlam, B. S. Mun, S. C. B. Myneni, A. Nilsson, H. Ogasawara, D. F. Ogletree, K. Pecher, M. Salmeron, D. K. Shuh, B. Tonner, T. Tyliszczak, T. Warwick, T. H. Yoon, *J. Electron Spectrosc. Relat. Phenom.* **2006**, *150*, 86.
[22] C. J. Powell, A. Jablonski, 1.1 ed., National Institute of Standards and Technology, Gaithersburg, MD, **2000**.
[23] J. Gustafson, A. Mikkelsen, M. Borg, E. Lundgren, L. Kohler, G. Kresse, M. Schmid, P. Varga, J. Yuhara, X. Torrelles, C. Quiros, J. N. Andersen, *Phys. Rev. Lett.* **2004**, *92*, 126102.
[24] C. T. Campbell, *Phys. Rev. Lett.* **2006**, *96*, 066106.

